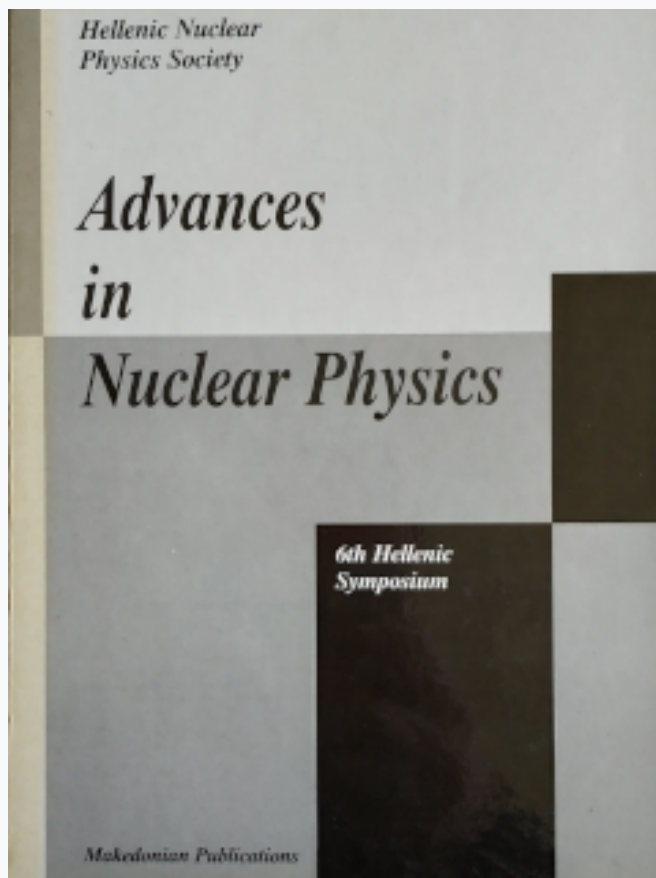


## Annual Symposium of the Hellenic Nuclear Physics Society

Τόμ. 6 (1995)

HNPS1995



### High Spin Structure of $^{122}\text{Xe}$

M. Serris, - et al.

doi: [10.12681/hnps.2923](https://doi.org/10.12681/hnps.2923)

#### Βιβλιογραφική αναφορά:

Serris, M., & et al., -. (2020). High Spin Structure of  $^{122}\text{Xe}$ . *Annual Symposium of the Hellenic Nuclear Physics Society*, 6, 140–151. <https://doi.org/10.12681/hnps.2923>

# High Spin Structure of $^{122}\text{Xe}$

M.Serris <sup>a</sup>, R.Vlastou <sup>a</sup>, C.T.Papadopoulos <sup>a</sup>, C.A.Kalfas <sup>b</sup>,  
N.Fotiades <sup>b</sup>, S.Harissopoulos <sup>b</sup>, S.Kossionides <sup>b</sup>, M.A.Riley <sup>c</sup>,  
J.Simson <sup>c</sup>, E.Paul <sup>c</sup>, J.F.Sharpey-Schafer <sup>c</sup> and P.J.Twin <sup>c</sup>

<sup>a</sup> *National Technical University of Athens 157 80, Greece*

<sup>b</sup> *Institute of Nuclear Physics, NCSR "Democritos", GR 153 10, Greece*

<sup>c</sup> *Oliver Lodge Laboratory, University of Liverpool, P.O. Box 147 Liverpool L69  
3BX, U.K.*

---

## Abstract

High spin states in the isotope  $^{122}\text{Xe}$  were populated using the reaction  $^{96}\text{Zn} (^{30}\text{Si}, 2n) ^{122}\text{Xe}$  at a beam energy of 135 MeV. The subsequent  $\gamma$ -ray deexcitation was studied using  $\gamma$ -ray spectroscopic methods. The analysis of  $\gamma$ - $\gamma$  coincidences has revealed two new structures of competing dipole and quadrupole transitions. The highest states of a positive parity band provide characteristics consistent with an approach to band termination.

---

## 1 Introduction

There exist two basic mechanisms by which the angular momentum of deformed nuclei can be generated. According to the first mechanism, angular momentum can be gained from the collective rotation of all nucleons of the deformed nucleus about an axis perpendicular to its symmetry axis. According to the second mechanism the angular momentum increases from the summed spin contributions of individual nucleons which are aligned all in the same direction. In the former case the pairs of valence nucleons in a prolate nucleus outside the closed shell are obliged by the Coriolis and centrifugal forces to break and to follow equatorial orbits around the rotation axis. This leads to the allignment of their spin with the rotation axis. In this case, if the number of nucleons participating in this allignment of spins is large enough, the nucleus can eventually take on an oblate shape. This shape change from collective prolate to non-collective oblate can be associated with the band termination concept [2]. The neutron deficient  $A \sim 120$  nuclei are good candidates for this band termination phenomenon, due to the limited number of valence nucleons

which can be aligned at high spin. Indeed, band termination changing effects from collective rotation to single particle motion have recently been observed in  $^{122}\text{Xe}$  [13],  $^{118}\text{Xe}$  [5] and a series of Iodine isotopes  $^{117,119,121}\text{I}$  [8], [9], [11].

Considerable interest in this  $A \sim 120$  region also centers on the new  $\Delta I=1$  structures which have recently been reported in  $^{126}\text{Ba}$  [16],  $^{128}\text{Ba}$  [10],  $^{132}\text{Ba}$  [6] and  $^{126}\text{Xe}$  [7]. These structures are characterized by strong dipole  $\Delta I=1$  transitions compared to weak  $\Delta I=2$  crossover ones and in most cases they have not been connected to the lower lying states. Large B(M1) transitions can be associated to high - K proton configurations for the interpretation of these structures coupled to neutron configurations to reproduce the angular momentum of the structures, where available. Another common feature of these structures is the kinematic moment of inertia with nearly the same dependence and same characteristics for all nuclei.

In this work preliminary results in  $^{122}\text{Xe}$  will be presented which exhibit characteristic properties expected for terminating bands, as well as new structures of competing dipole and quadrupole transitions.

## 2 Experimental Method

Excited states of  $^{122}\text{Xe}$  were populated through the compound nuclear reaction  $^{96}\text{Zr}(^{30}\text{Si},4n)^{122}\text{Xe}$  at a beam energy of 135 MeV. The beam was provided by the tandem Van de Graaf accelerator at the Nuclear Structure Facility at Daresbury Laboratory. The target was a  $500 \mu\text{g}/\text{cm}^2$   $^{96}\text{Zr}$  on  $10 \text{ mg}/\text{cm}^2$   $^{197}\text{Au}$  backing. The  $\gamma$ -rays were detected with the EUROGAM detector array, consisted of 45 BGO escape-suppressed Ge detectors. The Ge detectors were of high- efficiency (65 ~ 80 % relative to a  $3'' \times 3''$  NaI(Tl) crystal at 1.33 MeV) and located at an average 21.5 cm from the target position. Suppressed Ge data were recorded when 6 or more unsuppressed Ge detectors were in coincidence within a time coincidence window of 50 ns. Events with a  $\gamma$ -ray fold greater than or equal to 3 were unfolded into double  $\gamma$ - $\gamma$  events and incremented into a symmetrized  $\gamma$ - $\gamma$  matrix. This matrix contained approximately  $2 \times 10^9$  events. Gamma-gamma matrices gated by known transitions of  $^{122}\text{Xe}$  were also constructed to produce clean spectra.

Angular-correlation information was obtained from the EUROGAM data which helped to determine the multipolarity of the transitions by using the coincidence spectra from detectors at  $158^\circ$  and  $\sim 90^\circ$  relative to the beam direction. The DCO ratios of the intensities  $\frac{I(158^\circ, 90^\circ)}{I(90^\circ, 158^\circ)}$  were determined with  $I(\theta_1, \theta_2)$  being the intensity of  $\gamma$ -rays in a detector at angle  $\theta_1$  when gated on a detector at angle  $\theta_2$ . This ratio is expected to be close to 1 for stretched-quadrupole



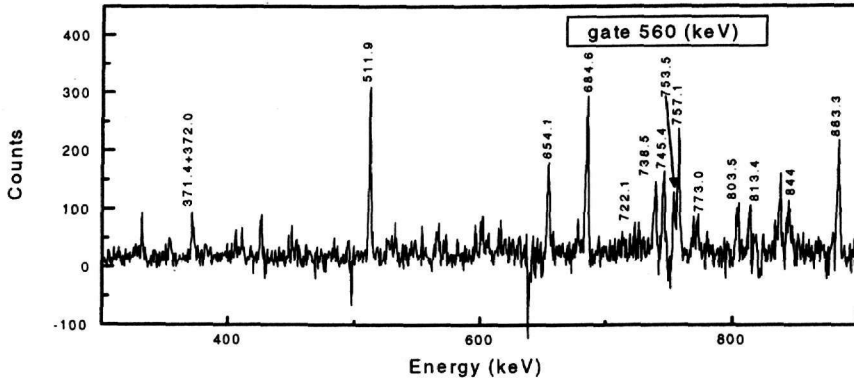


Fig 2. Transitions in coincidence with the 560 keV  $\gamma$ -ray.

### 3 Level Scheme

The level scheme of  $^{122}\text{Xe}$  has previously been studied by Hattula et al. [4] as well as by Simpson et al. [13] and Timmers et al. [14]. In the present work the decay scheme of  $^{122}\text{Xe}$  has been enriched and new structures have been observed, as it is shown in fig. 1. The observed bands have been labelled in order to facilitate the discussion.

The  $\gamma$  band has been established by Hattula et al. [4] up to spin  $11^+$  and in the present work it has been extended up to spin  $14^+$ . The  $9^+$  to  $7^+$  transition detected by Hattula et al. to be at an energy of 755 keV, was observed in this work as a double peak with energies 757.1 keV and 753.5 keV deexciting the  $9^+$  to  $7^+$  and  $13^+$  to  $11^+$  levels, respectively. All the transitions placed in this band can be seen in the coincidence spectrum, gated on the 559.8 and 560.4 keV transitions and is presented in fig. 2.

The GS, S,  $S^a$ ,  $S^b$  bands have been observed by Timmers et al. [14] up to spin  $24^+$  for the  $S^b$  and  $25^+$  for the  $S^a$  band. In the present study the GS, S and  $S^b$  bands have been confirmed, while above the  $S^a$  band, a new structure has been established, which extends up to spin  $29^+$  and carries an intensity of about 12 % of that of the lowest 331.3 keV transition. The DCO ratios extracted for the 566.1, 460.5, 452.8 keV transitions suggest that these  $\gamma$ -rays are stretched dipole transitions, while the 1069.0 keV is a stretched quadrupole transition. The multipolarity of the  $\gamma$ -rays helped to determine the spin and parity of the

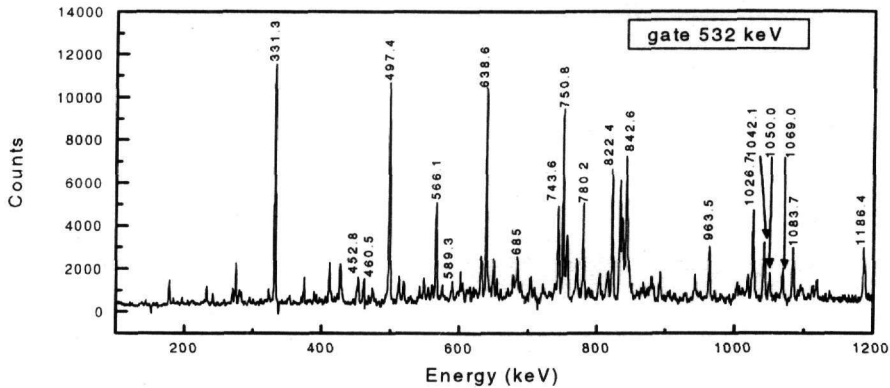


Fig 3. Transitions in coincidence with the 532 keV ( $23^+ \rightarrow 22^+$ )  $\gamma$ -ray.

levels of this structure. The  $\gamma$ -rays in  $S^a$  band are seen in fig. 3 which shows the spectrum gated on the 532 keV transition.

The P1 band has previously been observed by Timmers et al. [14] up to spin  $32^+$  with the 304.6 keV transitions on the top, built on the  $30^+$  state. In this study the data allowed the rearrangement of the transitions so that the 1342 keV transition deexcites the  $32^+$  level while the 304.6 and 882.7 keV  $\gamma$ -rays feed the  $28^+$  state. As shown in fig. 4 the 1187.3 keV transition is not seen in the coincidence spectrum gated on the 304 keV transition.

Another new structure, labelled P2, of twelve transitions built below the 9172.8 keV level has been established, with an intensity of about 15 % of that of the 331.3 keV transition. The P2 structure decays to the 5236.8 level of the N1 band through the 269.5 and 619.1 as well as 274.2 and 614.5 keV transitions. This decay out to the N1 band carries about half of the intensity of P2 structure. The rest of the intensity of this structure could be fragmented into several paths feeding the GS and S band since the levels of the S band up to spin  $14^+$  can be seen in  $\gamma$ -ray spectra gated on transitions of the P2 structure. The DCO ratios which have been measured for the 852.2, 868.3 and 834.1 keV suggest that these  $\gamma$ -rays are stretched quadrupole transitions, and the 410.9, 426.6, 425.6, 450.4, 545.2 keV decays are stretched dipole transitions. So the spin and parity of this structure could be defined.

Useful information about the form of this structure can be extracted from the spectra gated on the 269 and 916 keV transitions. In the coincidence spectrum of 269 keV in fig. 5 we observe that the 269 keV transition coincides with all

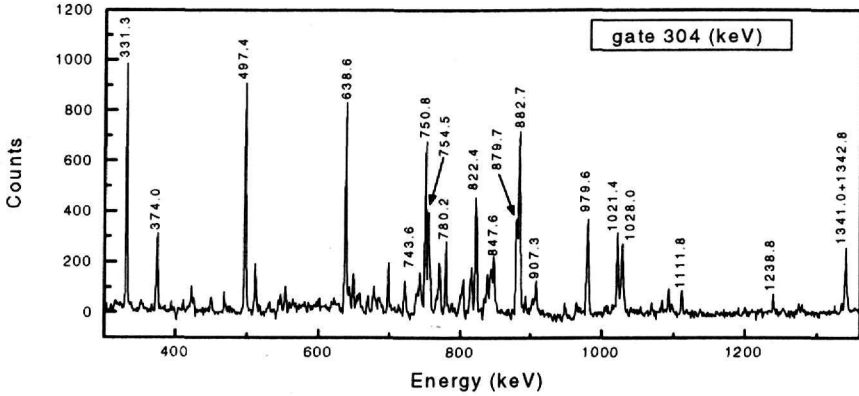


Fig 4. Transitions in coincidence with the 304 keV ( $30^+ \rightarrow 29^+$ )  $\gamma$ -ray.

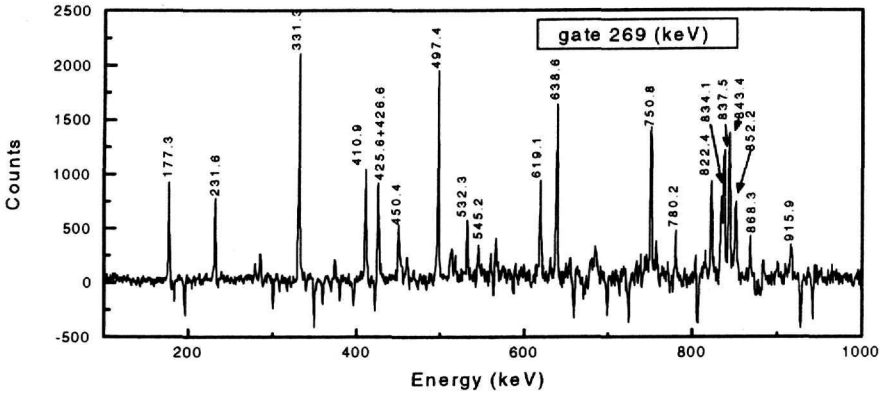


Fig 5. Transitions in coincidence with the 269 keV  $\gamma$ -ray.

the others except the 274 and 614 keV  $\gamma$ -rays. In the coincidence spectrum of 916 keV in fig. 6 we observe that the 916 keV transition is in coincidence with all the rest  $\gamma$ 's with the exception of the 532 and 834 keV transitions.

The N1 band has been reported by Hattula et al. [4] to be built on a level 4046 keV with spin of  $10^-$  or  $11^-$  and deexcites to the  $10^+$  state of the GS band through the 1007.2 keV E1 transition. In the present study the 1007.2 keV transition was built on the  $12^+$  level of the GS band, so the energy, spin

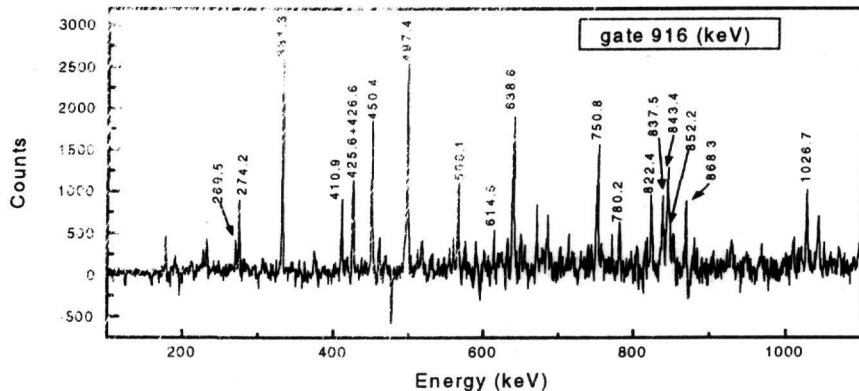


Fig 6. Transitions in coincidence with the 916 keV ( $23^+ \rightarrow 21^+$ )  $\gamma$ -ray.

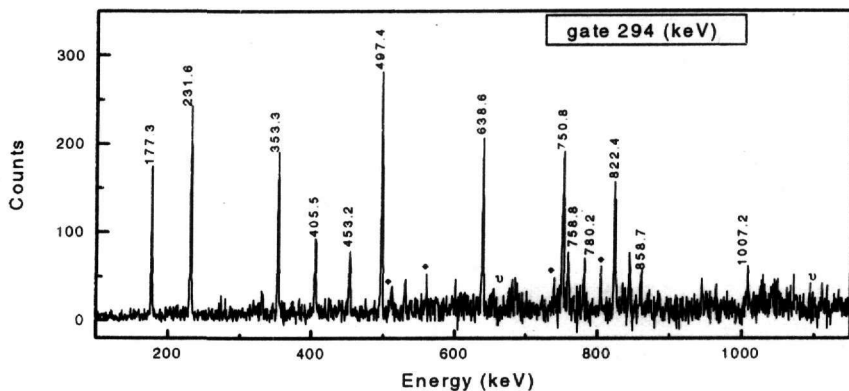


Fig 7. Transitions in coincidence with the 294 keV ( $15^- \rightarrow 14^-$ )  $\gamma$ -ray.

and parity of the band head level was defined to be 4827.9 keV with  $\Gamma=12^-$ . The DCO ratios of the 177.3, 231.6, 294.8, 353.3, 405.5 and 453.2 keV transitions indicate  $L=1$  multipolarity, which helps to deduce the spin and parity of the other levels of this band. Most of the transitions placed in N1 band can be seen in the coincidence spectrum, gated on the 294.8 keV transition which is present in fig. 7. In this spectrum the peaks marked with an asterisk correspond to the transitions of the  $\gamma$ -band up to the  $12^+$  state. The linking transitions to this band, however, could not be defined. The  $12^+$  state of the P1 band is also seen by the N1 band through the 675.6 keV transition which is marked

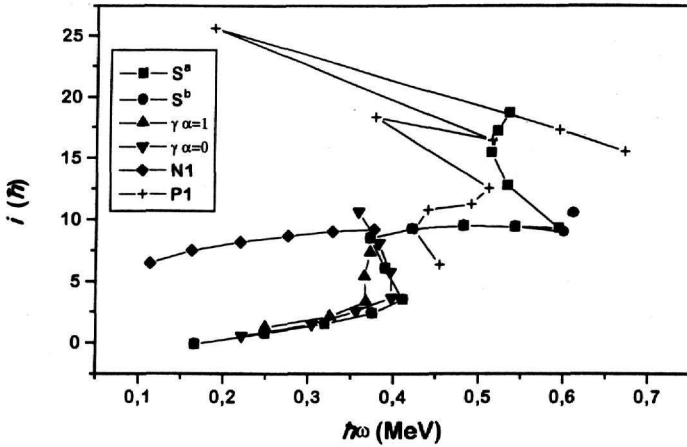


Figure 8: Aligned angular momenta for the GS,  $S^a$ ,  $S^b$ , P1, N1 and  $\gamma$  bands in  $^{122}\text{Xe}$ . A reference based on the moment of inertia parameters  $J_0 = 9MeV^{-1}\hbar^2$  and  $J_1 = 33MeV^{-3}\hbar^4$  has been used.

in the spectrum with a triangle together with the 1111.8 keV  $\gamma$ -ray.

#### 4 Discussion

In order to discuss the structure and properties of the bands the experimental aligned angular momenta  $i(\omega)$  have been extracted as a function of frequency  $\omega$  and are presented in fig. 8. The yrast  $\Delta I=2$  GS band is built on a positive parity  $0^+$  state with a possible ground state configuration  $\pi[(d_{5/2}^2, (g_{7/2}^2)]\nu[(s_{1/2}^2, (h_{11/2}^2)]$  as proposed by Timmers et al. [14]. The first crossing between the GS and S bands occurs at  $\hbar\omega = 0.38$  MeV and the nucleus gains an aligned angular momentum  $i_{exp} = 6\hbar$ . This crossing has been associated by Hattula et al. [4] with the  $\nu(h_{11/2}^2)$  alignment.

The  $\gamma$ -vibrational band is built on a positive parity  $2^+$  state for the  $\alpha=0$  signature and  $3^+$  state for the  $\alpha=1$  one.  $\gamma$ -vibrational bands have also been observed in the neighbouring  $^{118}\text{Xe}$  and  $^{120}\text{Xe}$  nuclei [15]. All these  $\gamma$ -bands exhibit similar characteristics. They are all built at low excitation energy and the  $\alpha=0$  branch is crossed by an aligned configuration connected to a positive

parity band, the P1 band in the case of  $^{122}\text{Xe}$ , which feeds both the yrast and the  $\gamma$ -band. In addition, the  $\alpha=1$  sequence of the  $\gamma$ -bands in the three isotopes exhibit a shift of the  $\nu(h_{\perp/2})^2$  crossing to lower frequencies than the yrast band. In the alignment plots of  $^{122}\text{Xe}$  in fig. 8  $\gamma$ -band is seen to follow the behavior of the ground state band, but the  $\nu(h_{\perp/2})$  backbend in the  $\alpha=1$  sequence occurs at  $\hbar\omega = 0.36$  MeV, while the  $\alpha=0$  one experiences the bandcrossing at  $\sim 0.38$  MeV like the yrast band. This shift could be attributed to the fact that the  $\gamma$ -band is effectively more triaxial than the yrast band [15].

The N1 band is characterized by strong  $\Delta I=1$  transitions and comparatively weak  $\Delta I=2$  crossover transitions. Experimental values of  $\frac{B(M1)}{B(E2)}$  ratios are currently been extracted and are found to be of the order of  $6 - 8 \frac{b^2}{e^2 b^2}$ . These properties suggest high - K proton configuration for the assignment of this band. Similar structures have also been observed in the neighbouring nuclei  $^{132}\text{Ba}$  [6] and  $^{122}\text{Ba}$ ,  $^{126}\text{Ba}$ ,  $^{128}\text{Ba}$ ,  $^{126}\text{Xe}$  [3], which however have not always been connected to the GS band so their spin and excitation energy are not defined. In this reference [3], an effort was tried to interpret these bands within the framework of the tilted cranking model, but the calculated branching ratios were too large compared to the experimental ones. Another interesting feature of these structures is the behaviour of the kinematic moment of inertia  $J^{(1)}$  with respect to the rotational frequency  $\omega$ . A plot of  $J^{(1)}$  as a function of  $\omega$  is presented in fig. 9 for  $^{122}\text{Xe}$  as well as for  $^{126}\text{Ba}$  and  $^{132}\text{Ba}$  where the spin of the  $\Delta I=1$  structures is known. The moment of inertia in these three isotopes exhibit a striking similarity suggesting that these  $\Delta I=1$  structures are characterized by similar configurations. If we compare the values  $J^{(1)}$  with the moment of inertia of a classical rigid rotor, which for an expected deformation  $\epsilon \simeq 0.2 - 0.3$  is  $J_{rigid} \simeq 44 - 46(\frac{\hbar^2}{MeV})$ , we see that  $J^{(1)}$  is larger than  $J_{rigid}$  for small values of  $\omega$  and becomes  $J_{rigid}$  for higher values of  $\omega$ . This can be attributed to the presence of a relatively constant quasiparticle alignment, see fig. 8 and ref. [1]

The P1 band experiences a crossing with GS band at  $\hbar\omega = 0.46$  MeV and the nucleus gains an aligned angular momentum  $i_{exp} = 7\hbar$ , see fig. 8. This crossing has been associated by Timmers et al. [14] with the  $\pi(h_{\perp/2})^2$  alignment, while the up-bend at  $\hbar\omega = 0.51$  MeV has been interpreted as the starting of the alignment of the first two  $\nu(h_{\perp/2})^2$  quasi neutrons.

At higher spin the rotational character gives place to a rather irregular behaviour, which could be interpreted as an approach to band termination. In order to analyze this behaviour a plot of excitation energies for the P1 band in  $^{122}\text{Xe}$  with respect to a rigid rotor term is presented in fig. 10. For the highest states of this band a down - sloping in  $\gamma$ -ray energies appears in the figure. This behaviour can be understood in terms of an approach to band termination or a change in shape from well deformed prolate to weakly deformed

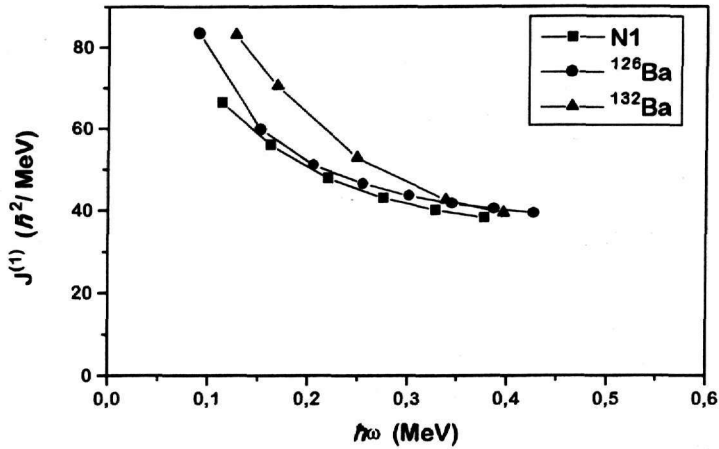


Figure 9: Kinematic moment of inertia  $J^{(1)}$  of the N1 band in  $^{122}\text{Xe}$  compared with similar bands in heavier even Ba nuclei.

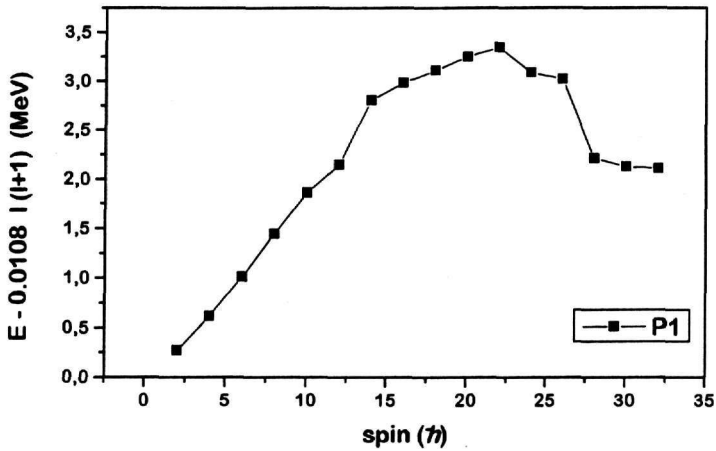


Figure 10: The excitation energies  $E$  relative to a rigid rotor reference for the positive parity states in band P1, as a function of angular momentum.

oblate [12]. This is due to the fact that when approaching termination, the spin is expected to be gained by requiring a relatively small amount of energy. Therefore if one plots the excitation energy  $E(I)$  as a function of spin, relative to a rigid - rotor reference, the levels associated with a terminating band sequence should be down - sloping [12]. The possible terminating configuration could be  $\pi[(h_{\frac{11}{2}})^2(g_{\frac{7}{2}}d_{\frac{5}{2}})^2]_{16^+} \nu[(h_{\frac{11}{2}})^4]_{16^+}$  which results to  $32^+$  spin [14].

The S band is found to split above spin  $20^+$  into two decay paths, which shows behaviour of single particle states. The  $S^a$  path, however, has been extended in the present work up to spin  $29^+$  and exhibits features of weak collectivity with competing dipole and quadrupole transitions. In addition, the P2 structure observed in this work shows similar properties of dipole transitions competing favourably with quadrupole crossover ones.  $\frac{B(M1)}{B(E2)}$  experimental ratios for bands  $S^a$ , P2 and N1 are currently under investigation. There is an indication, however, that these values are high, varying between  $4 - 10 \frac{10^2}{e^2 b^2}$ , which indicates that the configurations of these structures are built on high - K proton orbitals.

In summary, the level scheme of  $^{122}\text{Xe}$  has been extended and enriched compared to previous works. The behaviour and configuration of the bands have been discussed. In addition, two new structures of competing dipole and quadrupole transitions have been observed and their properties have been compared with similar structures in neighbouring nuclei.

## References

- [1] R. Bengtsson and S. Frauendorf Nucl. Phys. A327 (1979) 139
- [2] A. Bohr, B R Mottelson Physica Scripta 10A (1974) 13
- [3] F. Dönau et al. Nucl. Phys. A584 (1995) 241
- [4] J. Hattula et al. Nucl. Phys. 13 (1987) 57
- [5] S. Juutinen et al. Z. Phys. A338 (1991) 365
- [6] S. Juutinen et al. Phys. Review C52 (1995) 2946
- [7] W. Lieberz et al. Z. Phys. A330 (1988) 221
- [8] Y. Liang et al. Phys. Rev. C44 (1991) R578
- [9] Y. Liang et al. Phys. Rev. C45 (1992) 1041

- [10] U. Neuneyer et al. Z. Phys. A336 (1991) 245
- [11] E. S. Paul J. Phys. G: Nucl. Part. Phys. 19 (1993) 913
- [12] I. Ragnarson et al. Physica Scripta 34 (1986) 651
- [13] J. Simpson et al. Phys. Lett. B262 (1991) 388
- [14] H. Timmers et al. J. Phys. G: Nucl. Part. Phys. 20 (1994) 287
- [15] S. Törmänen et al. Nucl. Phys. A572 (1994) 417
- [16] D. Ward et al. Nucl. Phys. A529 (1991) 315